Iranian Journal of Science (2023) 47:1299–1311
https://doi.org/10.1007/s40995-023-01490-y

RESEARCH PAPER

A Reduced-Order Finite Difference Scheme Based on POD for Fractional Stochastic Advection–Diffusion Equation

Z. Soori[1] · A. Aminataei[1] · D. Baleanu[2,3]

Received: 24 December 2022 / Accepted: 4 June 2023 / Published online: 6 July 2023

Abstract
This article introduces a new scheme for the fractional stochastic advection–diffusion equation (FSA-DE) in time where the fractional term is expressed in Caputo sence of order α $(0<\alpha<1)$. First, an L1 approximation is employed to estimate the Caputo derivative. Then, the spatial derivative is approximated by a second-order finite difference scheme. Moreover, we combine the implicit finite difference (IFD) scheme with the proper orthogonal decomposition (POD) method to reduce the used CPU time. In other words, the POD based reduced-order IFD scheme is obtained. The proposed scheme can be regarded as the modification of the exiting work (Mirzaee et al. in J Sci Technol Trans Sci 45:607–617, 2001). The numerical results are provided to confirm the feasibility and efficiency of the proposed method.

Keywords Fractional stochastic advection–diffusion equation · Implicit finite difference scheme · Proper orthogonal decomposition method · Reduced implicit finite difference scheme

Mathematics Subject Classification 37L55 · 65M06 · 35R11

1 Introduction

Considering (Oksendal 2000), the question arises why one should learn more about stochastic calculus? Stochastic partial differential equations (SPDEs) play an important role in a wide range of active research in mathematics, chemistry, fluid mechanics, microelectronics, theoretical physic and finance (Ren and Tian 2022; Li et al. 2019; Yoon et al. 2022).

Fractional differential equations have attracted increasing attention by reason of their application in several field including mathematics, fluid mechanics, physics, chemistry, hydrology and finance.

Despite the enormous number of studies fractional differential equations of deterministic type, a few papers exist in connection with fractional stochastic equations (FSDEs) especially Caputo time fractional derivative. Previous studies have been limited to the existence and uniqueness of mild solution. Interesting papers for existence and uniqueness are found in Ciprian (2013); Pedjeu and Ladde (2012); Sakthivel et al. (2013).

In the past few years, there has been a big development in numerical solution of SPDEs. For example, authors of Sweilam et al. (2020) solved the stochastic advection–diffusion equation of fractional order in space by fourth-order finite difference scheme of Itô type. They used Fourier analysis to prove stability and convergence of presented scheme similar to Roth (2002). In Zou (vvv), a Galerkin finite element method was considered for time fractional stochastic diffusion equation with multiplicative noise. A numerical method for the nonlinear stochastic reaction–diffusion equation of fractional order in time was carried out in Liu and Yang (2021) wherein mixed finite element and BDF2-θ were considered to discretize in spatial and temporal directions, respectively. Kamrani

✉ Z. Soori
zsoori@mail.kntu.ac.ir

A. Aminataei
ataei@kntu.ac.ir

D. Baleanu
dumitru@cankaya.edu.tr

[1] Department of Mathematics, K. N. Toosi University of Technology, Tehran, Iran

[2] Department of Mathematics, Cankaya University, 06530 Ankara, Turkey

[3] Lebanese American University, Beirut, Lebanon

(2015) investigated the numerical solution of FSDEs using Galerkin method based on Jacobi polynomials. The main aim of Zhou et al. (2021) was to develop a fourth-order central difference scheme and the semi-implicit Crank–Nicolson scheme for obtaining a new fully discrete scheme of space-fractional wave equation by additive and multiplicative noise. In Peng and Huang (2019), a nonlocal problem as backward was proposed for FSDEs wherein the eigenfunction expansion of the solution was reduced to an integral equation. Authors of He and Peng (2019) explained an approximate controllability for fractional stochastic wave equation of Riemann–Liouville type.

The POD technique has a long-standing history. It was derived from eigenvector analysis method which was initially proposed by K. Pearson in 1901. The POD (Holmes et al. 2012) was known as an efficient technique to decrease the degrees of freedom. The essential features of the POD based reduced are in the following two aspects, i.e., preserve the accuracy of numerical solutions and reduce the computational time. Known studies are reduced order for finite differences, finite element and finite volume element methods which are found in the book (Luo and Chen 2018). The POD method is needed more for scheme that are on fine grids. For example, there is more computation cost in the Richardson extrapolation algorithms on fine grids. Hence, we are able to use POD technique instead of parallel computing to overcome with this problem.

A finite element method combined with POD scheme for Tricomi-type equation of fractional order was considered in Liu et al. (2016). Authors of Abbaszadeh and Dehghan (2020); Xu and Zhang (2019); Zhang and Zhang (2018) presented some efficient compact finite difference schemes combined with POD for PDEs such as Riesz space-fractional diffusion equation of distributed-order type in two-dimensions, multidimensional parabolic equation and Korteweg–de Vries equation. Some reduced finite difference schemes based on POD scheme for parabolic and hyperbolic equations were utilized in Luo et al. (2009, 2016), Sun et al. (2010). Abbaszadeh et al. (2022) developed a fast and robust numerical formulation to simulate a system of fractional PDEs using a reduced-order method based upon the POD technique. Authors Dehghan and Abbaszadeh (2018a) combined the EFG method based on the RPIM (EFG-RPIM) with POD technique for solving two-dimensional solute transport problems. Fu et al. (2018) investigated a reduced order for fractional diffusion equation in time based on POD technique and disceret experimental interpolation method. Luo and Wang (2020) developed an extrapolation and finite difference schemes as reduced order by POD for diffusion-wave equation of time–space tempered type in two-dimensional case. The POD scheme was included in fluid dynamics as well, for example in Kunisch and Volkwein (2001, 2002) a Galerkin POD method for parabolic and general equations was utilized. For further details about POD method see (Abbaszadeh and Dehghan 2020; Abedini et al. 2021; Dehghan and Abbaszadeh 2017, 2018b; Luo et al. 2007, 2009, 2012).

In this article, we consider the FSA-DE in time as follows:

$$
\begin{aligned}
{}_0^{\mathrm{C}}\mathcal{D}_t^{\alpha}u(x,t) =&(\beta+\gamma\frac{dB(t)}{dt})\frac{\partial^2u(x,t)}{\partial x^2}+\sigma\frac{\partial u(x,t)}{\partial x}\\
&+f(x,t),\quad (x,t)\in(L_0,L)\times(0,T],
\end{aligned}
\tag{1}
$$

with the initial and boundary conditions:

$$
\begin{aligned}
u(x,0)&=\psi(x),\quad x\in[L_0,L],\\
u(L_0,t)&=\varphi_1(t),\quad t\in(0,T],\\
u(L,t)&=\varphi_2(t),\quad t\in(0,T],
\end{aligned}
$$

here ${}_0^{\mathrm{C}}\mathcal{D}_t^{\alpha}$ is the fractional derivative operator of Caputo type defined as

$$
\begin{aligned}
&{}_0^{\mathrm{C}}\mathcal{D}_t^{\alpha}u(x,t)\\
&\quad=\frac{1}{\Gamma(1-\alpha)}\int_0^t\frac{\partial^2u(x,t)}{\partial s^2}(t-s)^{-\alpha}\mathrm{d}s,\quad 0<\alpha<1,
\end{aligned}
$$

here, β,γ,σ are constants, $\psi(x),\varphi_1(t),\varphi_2(t)$ are the stochastic process defined on the propability space $(\Omega,\mathcal{F},\mathcal{P})$, $f(x,t)$ a known function and $u(x,t)$ is an unknown stochastic process which should be estimated. The term $B(t)$ denotes one-dimensional standard Brownian motion process which satisfy in the following properties:

1) $B(0)=0$.
2) For all $0\le s<t<T$, $B(t)-B(s)$ is random variable with variance $t-s$ and expectation zero. Therefore, $B(t)-B(s)\sim\sqrt{t-s}\mathcal{N}(0,1)$ denotes normal distribution with variance 1 and expectation zero.
3) For $0\le s<t<u<v<T$, the increments $B(t)-B(s)$ and $B(v)-B(u)$ are independent. We point that the Brownian motion is a function very commonly used in stochastic calculus. It is a continuous process but it is not a differentiable function.

In this paper, first, we employ the classical L1 formula to approximate the Caputo fractional derivative and then we discretize the spatial derivative using the second-order IFD scheme. Afterward, combination of POD technique and IFD scheme is considered for FSA-DE wherein POD-IFD is constructed. It can not be only reduced into a scheme with lower dimension number, but also guarantee high accuracy. The error analysis is discussed as well. What distinguishes the current paper from previous works is its numerical solution aspect. To our knowledge, the POD-IFD scheme has not ever applied to solve FSA-DE in

time. Although L1 is an elementary approach for Caputo fractional derivative, it produces efficient and reasonable results in terms of numerical convergence order and numerical stability in time direction compared to higher order schemes (Gao et al. 2014; Mirzaee et al. 2020).

The outline of this article is arranged as follows: In Sect. 2, the IFD scheme is employed to approximate spatial derivatives and the classical L1 formula to discretize time Caputo fractional derivative. In Sect. 3, we turn to the POD method and then we combine the POD technique with the IFD scheme. In Sect. 4, the analysis of errors for the IFD and RIFD schemes is discussed. in Sect. 5, two numerical examples have been given to verify the accuracy and efficiency of our proposed method. Finally, some conclusions are drawn in Sect. 6.

2 Numerical Scheme

This section is devoted to establish difference approximation to the Eq. (1). For this purpose, we define $x_i = L_0 + ih$, for $i = 0, 1, \ldots, M$ and $t_n = n\tau$ for $n = 0, 1, \ldots, N$, wherein $h = \frac{L-L_0}{M}$ and $\tau = \frac{T}{N}$ be the spatial and temporal step sizes, respectively, where M, N are two given positive integers. For any grid function $u = \{u_i^n | 0 \le i \le M, 0 \le n \le N\}$, denote

$$\hat{\delta}_x u_i^n = \frac{u_{i+1}^n - u_{i-1}^n}{2h}, \qquad \delta_x^2 u_i^n = \frac{u_{i+1}^n - 2u_i^n + u_{i-1}^n}{h^2}, \qquad \frac{dB}{dt} = \frac{B_n - B_{n-1}}{\tau}. \tag{2}$$

Here, ${}_0^C\mathcal{D}_t^\alpha u(x, t_n)$ can be approximated by the L1 formula (Zhuang and Liu 2006) as follows:

$$\begin{aligned} {}_0^C\mathcal{D}_t^\alpha u(x, t_n) &= \frac{1}{\Gamma(1-\alpha)} \sum_{k=0}^{n-1} \int_{t_k}^{t_{k+1}} \frac{\partial u(x,s)}{\partial s} (t_n - s)^{-\alpha} \mathrm{d}s \\ &\approx \frac{1}{\Gamma(1-\alpha)} \sum_{k=0}^{n-1} \frac{u(x, t_{k+1}) - u(x, t_k)}{\tau} \\ &\quad \int_{t_k}^{t_{k+1}} (t_n - s)^{-\alpha} \mathrm{d}s \\ &= \frac{\tau^{-\alpha}}{\Gamma(2-\alpha)} \sum_{k=0}^{n-1} a_k \left[u(x, t_{n-k}) - u(x, t_{n-k-1}) \right] \\ &\quad + O(\tau^{2-\alpha}), \end{aligned} \tag{3}$$

Lemma 1 *The coefficients* $a_k = (k+1)^{1-\alpha} - (k)^{1-\alpha}, \quad k = 0, 1, \ldots, n-1$, *satisfy*

(1) $1 = a_0 > a_1 > a_2 > \ldots > a_k \ldots \longrightarrow 0$,
(2) $(1-\alpha)(k+1)^{-\alpha} < a_k < (1-\alpha)(k)^{-\alpha}$.

Substituting Eqs. (2) and (3) into Eq. (1), the IFD is obtained as follows:

$$\begin{aligned} &\frac{\tau^{-\alpha}}{\Gamma(2-\alpha)} \left[u_i^n - \sum_{k=1}^{n-1} (a_{n-k-1} - a_{n-k}) u_i^k - a_{n-1} u_i^0 \right] \\ &= \left(\beta + \gamma \frac{B_n - B_{n-1}}{\tau} \right) \frac{u_{i+1}^n - 2u_i^n + u_{i-1}^n}{h^2} \\ &\quad + \sigma \frac{u_{i+1}^n - u_{i-1}^n}{2h} + f_i^n, \\ &\quad i = 1, 2, \ldots, M-1, \quad n = 1, 2, \ldots, N. \end{aligned} \tag{4}$$

After simplification, we can rewrite the Eq. (4) as follows:

$$\begin{aligned} &\left[-\frac{\mu}{h^2} \left(\beta + \gamma \left(\frac{B_n - B_{n-1}}{\tau} \right) \right) - \frac{\mu\sigma}{2h} \right] u_{i+1}^n \\ &\quad + \left[1 + \frac{2\mu}{h^2} \left(\beta + \gamma \left(\frac{B_n - B_{n-1}}{\tau} \right) \right) \right] u_i^n \\ &\quad + \left(-\frac{\mu}{h^2} \left(\beta + \gamma \left(-\frac{B_n - B_{n-1}}{\tau} \right) \right) + \frac{\mu\sigma}{2h} \right) u_{i-1}^n \\ &\quad = \sum_{k=1}^{n-1} (a_{n-k-1} - a_{n-k}) u_i^k - a_{n-1} u_i^0 + \mu f_i^n, \\ &\quad i = 1, 2, \ldots, M-1, \end{aligned} \tag{5}$$

where $\mu = \tau^\alpha \Gamma(2-\alpha)$. In order to facilitate computations, the difference scheme (5) can be represented to the following matrix–vector multiplication:

$$\begin{cases} K_n u^1 = \mu F^1 + G^1, \\ K_n u^n = c_1 u^{n-1} + c_2 u^{n-2} + \ldots \\ \quad + c_{n-1} u^{n-1} + a_{n-1} u^0 + \mu F^n + G^n, \qquad n > 1. \end{cases} \tag{6}$$

Notice that K_n, F^n and G^n are tridiagonal matrices defined by:

$$\begin{aligned} K_n &= \mathrm{tri} \left[-\frac{\mu}{h^2} \left(\beta + \gamma \left(\frac{B_n - B_{n-1}}{\tau} \right) \right) - \frac{\mu\sigma}{2h}, 1 \right. \\ &\quad + \frac{2\mu}{h^2} \left(\beta + \gamma \left(\frac{B_n - B_{n-1}}{\tau} \right) \right), \\ &\quad \left. - \frac{\mu}{h^2} \left(\beta + \gamma \left(\frac{B_n - B_{n-1}}{\tau} \right) \right) + \frac{\mu\sigma}{2h} \right], \\ F^n &= \left[f_1^n, f_2^n, \ldots, f_{M-1}^n \right]^T, \\ G^n &= \left[-\frac{\mu}{h^2} \left(\beta + \gamma \left(\frac{B_n - B_{n-1}}{\tau} \right) \right) + \frac{\mu\sigma}{2h}, 0, \ldots, 0, \right. \\ &\quad \left. - \frac{\mu}{h^2} \left(\beta + \gamma \left(\frac{B_n - B_{n-1}}{\tau} \right) \right) - \frac{\mu\sigma}{2h} \right]^T, \end{aligned}$$

and $c_n = a_{n-1} - a_n (n = 1, 2, \ldots, N)$. The approximate solutions $\{u_i^n\}$ $(i = 1, 2, \ldots, M-1)$ are obtained from solving IFD scheme (6).

Theorem 2 *The IFD scheme (6) has a unique solution.*

For any possible values of μ, β, γ, τ and h, the coefficient matrix K_n is strictly diagonal dominant, so it is non-singular, thus it is invertible. Consequently, the difference scheme (6) has a unique solution.

3 The RIFD Scheme Based on POD Method

We devote this section to employ the POD method for creating the RIFD scheme. Up to now, there have been different interpretations for the POD method. Three of the most methods are Karhunen–Loeve decomposition (KLD), the principal component analysis (PCA) and the singular value decomposition (SVD). In this article, we utilize the direct form of the POD based on SVD (Luo et al. 2016).

3.1 Formulate the POD Basis

Step 1. Form snapshots

For this aim, we choose first $G \ll N$ sequence of solutions $\{u_i^n\}_{n=1}^G$ from the N sequence of approximate solutions $\{u_i^n\}_{n=1}^N$ $(i = 1, 2, \ldots, M-1)$ of IFD (6).

$$S = \begin{pmatrix} u_1^1 & u_1^2 & \ldots & u_1^G \\ u_2^1 & u_2^2 & \ldots & u_2^G \\ \vdots & \vdots & \ddots & \vdots \\ u_M^1 & u_M^2 & \ldots & u_M^G \end{pmatrix}_{M-1\times G}, \tag{7}$$

Step 2. Apply the SVD form on Matrix S

$$S = U\begin{pmatrix} D_r & 0 \\ 0 & 0 \end{pmatrix}V^T,$$

where $D_r = \mathrm{diag}(\sigma_1, \sigma_2, \ldots, \sigma_r)$. The singular values σ_i can be arranged as $\sigma_1 \geq \sigma_2 \geq \ldots \geq \sigma_r > 0$ and $r = \mathrm{rank(S)}$. $U = U_{M-1\times M-1}$ and $V = V_{G\times G}$ are orthogonal matrices. The matrice $U = (\Phi_1, \Phi_2, \ldots, \Phi_{M-1})$ and $V = (\psi_1, \psi_2, \ldots, \psi_{M-1})$ include the eigenvalues with orthogonality property to the SS^T and S^TS, respectively, and also $\lambda_i = \sigma_i^2 (i = 1, 2, \ldots, r)$. We define a projection P_M by

$$P_M(S^G) = \sum_{j=1}^{m}(\Phi_j, S^g)\Phi_j, \qquad (g = 1, 2, \ldots, G), \tag{8}$$

where $S^g = \left[u_1^g, u_2^g, \ldots, u_{M-1}^g\right]$, besides, $m < r$ and (Φ_j, S^g) is inner product of vectors Φ_j and S^g. The following inequality for orthogonal projection is result:

$$\left|s^g - P_m(s^g)\right|_2 \leq \sigma_{m+1} = \sqrt{\lambda_{m+1}}. \tag{9}$$

The $\{\Phi_i\}_{i=1}^m$ is a set of optimal basis and $\Phi = (\Phi_1, \Phi_2, \ldots, \Phi_m)$ is a matrix created by the eigenvectors with property $\Phi^T\Phi = \mathrm{I}$. Now, we establish a RIFD scheme, if u_n of (6) is substituted by

$$\begin{aligned} P_m(u^n) &= \widehat{u}^n = \Phi w^n \\ &= \Phi_{(M-1)\times m}(w^n)_{m\times 1}, \qquad n = 0, 1, \ldots, N. \end{aligned} \tag{10}$$

Considering $\Phi^T\Phi = \mathrm{I}$, we obtain RIFD scheme as follows:

$$\begin{cases} Hw^1 = \mu H\Phi^T F^1 + \Phi^T B^1, \\ Hw^n = c_1 w^{n-1} + c_2 w^{n-2} + \ldots + c_{n-1}w^{n-1} \\ \quad + a_{n-1}w^0 + \mu\Phi^T F^n + \Phi^T B^n, \qquad n > 1, \end{cases} \tag{11}$$

where $H = \Phi^T K \Phi$. Having computed w^n from (11), we obtain POD optimal solution $\widehat{u}^n = \Phi w^n$. The RIFD only contains $m \times N$ equations, while IFD contains $(M-1) \times N$ equations (usually $m \ll M-1$). In fact, the number of degrees of freedom in RIFD scheme (11) reduces in comparision with IFD (6). Henece, we use RIFD method.

4 Error Estimation

This section is devoted in analyzing the errors of the IFD and RIFD solutions. First, we state the following remark and that which is basic in the whole theory.

5 Remark

Matrix K_n in IFD scheme (6) is not a symmetric tridiagonal matrix. By numerical computations, assume that each product of off-diagonal entires is strictly positive $b_i c_i$.

A transform matrix D define as follows:

$$D = \mathrm{diag}(\delta_1, \ldots, \delta_n),$$

and

$$\delta_i = \begin{cases} 1, & i = 1, \\ \sqrt{\dfrac{c_{i-1}\ldots c_1}{b_{i-1}\ldots b_1}}, & i = 2, \ldots n-1. \end{cases}$$

Based on bts (bts), a symmetric tridiagonal matrix J can be obtained as follows:

$$J = D^{-1}TD = \begin{pmatrix} a_1 & \mathrm{sgn}b_1\sqrt{b_1c_1} & & \\ & \mathrm{sgn}b_1\sqrt{b_1c_1} & a_2 & \mathrm{sgn}b_2\sqrt{b_2c_2} \\ & \ddots & \ddots & \ddots \\ & & & \\ & \mathrm{sgn}b_{n-1}\sqrt{b_{n-1}c_{n-1}} & & \\ & & & \\ & \mathrm{sgn}b_{n-1}\sqrt{b_{n-1}c_{n-1}} & & \\ & a_n & & \end{pmatrix}, \tag{12}$$

For simplicity, we assume that the entires of K_n define as follows:

Table 1 Comparison of approximate and exact solutions with $h = \tau = \frac{1}{200}$ of Experiment 1

x	Exact	Approximate			
		$\alpha = 0.2$	$\alpha = 0.4$	$\alpha = 0.6$	$\alpha = 0.8$
0.1	0.30901699	0.30904178	0.30904202	0.30904760	0.30903757
0.2	0.58778525	0.58783269	0.58783312	0.58784369	0.58782973
0.3	0.80901699	0.80908265	0.80908321	0.80909770	0.80908988
0.4	0.95105652	0.95113401	0.95113470	0.95115169	0.95116014
0.5	1.00000000	1.00008110	1.00008256	1.00010037	1.00013076
0.6	0.95105694	0.95113489	0.95113536	0.95115226	0.95120253
0.7	0.80901694	0.80908400	0.80908435	0.80909869	0.80915854
0.8	0.58778525	0.58783420	0.58783441	0.58784480	0.58789851
0.9	0.30901699	0.30904287	0.30904297	0.30904842	0.30908019

Table 2 Numerical convergence orders in spatial direction with $\tau = \frac{1}{100}$ for Experiment 1

α	h	L_∞	$C_h - Order$
0.25	$\frac{1}{10}$	8.2650×10^{-3}	–
	$\frac{1}{20}$	2.2813×10^{-3}	1.8572
	$\frac{1}{40}$	5.3933×10^{-4}	2.0806
	$\frac{1}{80}$	1.3220×10^{-4}	2.0284
0.5	$\frac{1}{10}$	8.4028×10^{-3}	–
	$\frac{1}{20}$	2.0929×10^{-3}	2.0054
	$\frac{1}{40}$	5.1753×10^{-4}	2.0158
	$\frac{1}{80}$	1.2555×10^{-4}	2.0434
0.75	$\frac{1}{10}$	8.3987×10^{-3}	–
	$\frac{1}{20}$	2.0744×10^{-3}	2.0175
	$\frac{1}{40}$	5.0072×10^{-4}	2.0506
	$\frac{1}{80}$	1.0772×10^{-4}	2.2167

Table 3 Numerical convergence orders in temporal direction with $\alpha = 0.5$ and $h = \frac{1}{100}$ for Experiment 1

τ	L_∞	$C_\tau - Order$
$\frac{1}{8}$	3.3085×10^{-3}	–
$\frac{1}{16}$	1.1448×10^{-3}	1.5311
$\frac{1}{32}$	2.6419×10^{-4}	2.1154
$\frac{1}{64}$	8.6190×10^{-5}	1.6160

$$T = \begin{pmatrix} a_1 & b_1 & & & & \\ c_1 & a_2 & b_2 & & & \\ & \ddots & \ddots & \ddots & & \\ & & & & & b_{n-1} \\ & & & & c_{n-1} & a_n \end{pmatrix}.$$

Now, matrices of J and T have the same eigenvalues. Here, matrix $K_n = T$. Now, we can obtain the eigenvalues of martix K_n by Thomas (1995):

$$\lambda_i(K_n) = 1 + \frac{2\mu}{h^2}\left(\beta + \gamma\left(\frac{B_n - B_{n-1}}{\tau}\right)\right) + 2\sqrt{\left(\frac{\mu^2}{h^4}\left(\beta + \gamma\left(\frac{B_n - B_{n-1}}{\tau}\right)\right)^2 - \frac{\mu^2\sigma^2}{4h^2}\right)} \cos\left(\frac{i\pi}{M}\right). \tag{13}$$

Theorem 3 *Let u^n be the solution of IFD scheme (6) and U^n the exact solution (6), then*

$$\|U^n - u^n\| \le C \sum_{k=1}^{n} \theta_{n,k}(h^2 + \tau^{2-\alpha}).$$

Proof From (6), we get:

$$K_n U^n = \sum_{k=1}^{n}(a_{n-k-1} - a_{n-k})U^k + a_{n-1}U^0 + \mu F^n + B^n + T^n, \quad 1 \le n \le N, \tag{14}$$

where T^n be the local truncation error. Let $e^n = U^n - u^n$ and $e^0 = 0$. Subtracting (6) from (14), we obtain:

$$K_n e^n = \sum_{k=1}^{n}(a_{n-k-1} - a_{n-k})e^k + T^n, \quad 1 \le n \le N.$$

Taking the inner product by e^n, we get:

$$(K_n e^n, e^n) = \sum_{k=1}^{n-1}(a_{n-k-1} - a_{n-k})(e^k, e^n) + (T, e^n), \quad 1 \le n \le N. \tag{15}$$

For any symmetric matrix R, the following property of Rayleigh–Ritz ratio (Horn and Johnson 1985) is obtained:

$$\lambda_{\min}(R) \le \frac{(Rv, v)}{(v, v)} \le \lambda_{\max}(R), \tag{16}$$

which vector v is in $\mathbb{R}^{M-1}$ and nonzero. Hence, we have:

$$\lambda_{\min}(K_n)\|e^n\|_2^2 = \lambda_{\min}(K_n)(e^n, e^n) \le (K_n e^n, e^n).$$

From the above equation, Eq. (15) becomes:

$$\|e^n\|_2 \le \frac{1}{\lambda_{\min}(K_n)}\left(\sum_{k=1}^{n-1}(a_{n-k-1} - a_{n-k})\|e^k\|_2 + \|T^n\|_2\right),$$
$$1 \le n \le N.$$

From (13), we have $\frac{1}{\lambda_{\min}(K_n)} \le 1$. Therefore, we obtain:

$$\|e^n\|_2 \le \left(\sum_{k=1}^{n-1}(a_{n-k-1} - a_{n-k})\|e^k\|_2 + \|T^n\|_2\right), \quad 1 \le n \le N.$$

By mathematical induction, we can obtain:

$$\|e^n\|_2 \le \sum_{k=1}^{n-1}\theta_{n,k}\|T^k\|_2, \quad 1 \le n \le N,$$

where

$$\theta_{n,j} = \sum_{k=1}^{n-j} C_{k+j-1}(a_{n-(k+j-1)-1} - a_{n-(j+j-1)})\theta_{k+j-1,j}.$$

From Eqs. (2) and (3), we obtain:

$$\|e^n\| \le C\sum_{k=1}^{n}\theta_{n,k}(h^2 + \tau^{2-\alpha}).$$

□

Theorem 4 *Suppose u^n and $\widehat{u}^n$ are the solution vectors of (6) and (11), respectively. We work on the assumption that the first $G \ll N$ sequence of solutions $\{u_i^n\}_{n=1}^G$ are from the N sequence solutions $\{u_i^n\}_{n=1}^N, i = 1, 2, \ldots, M-1$, as snapshots, then*

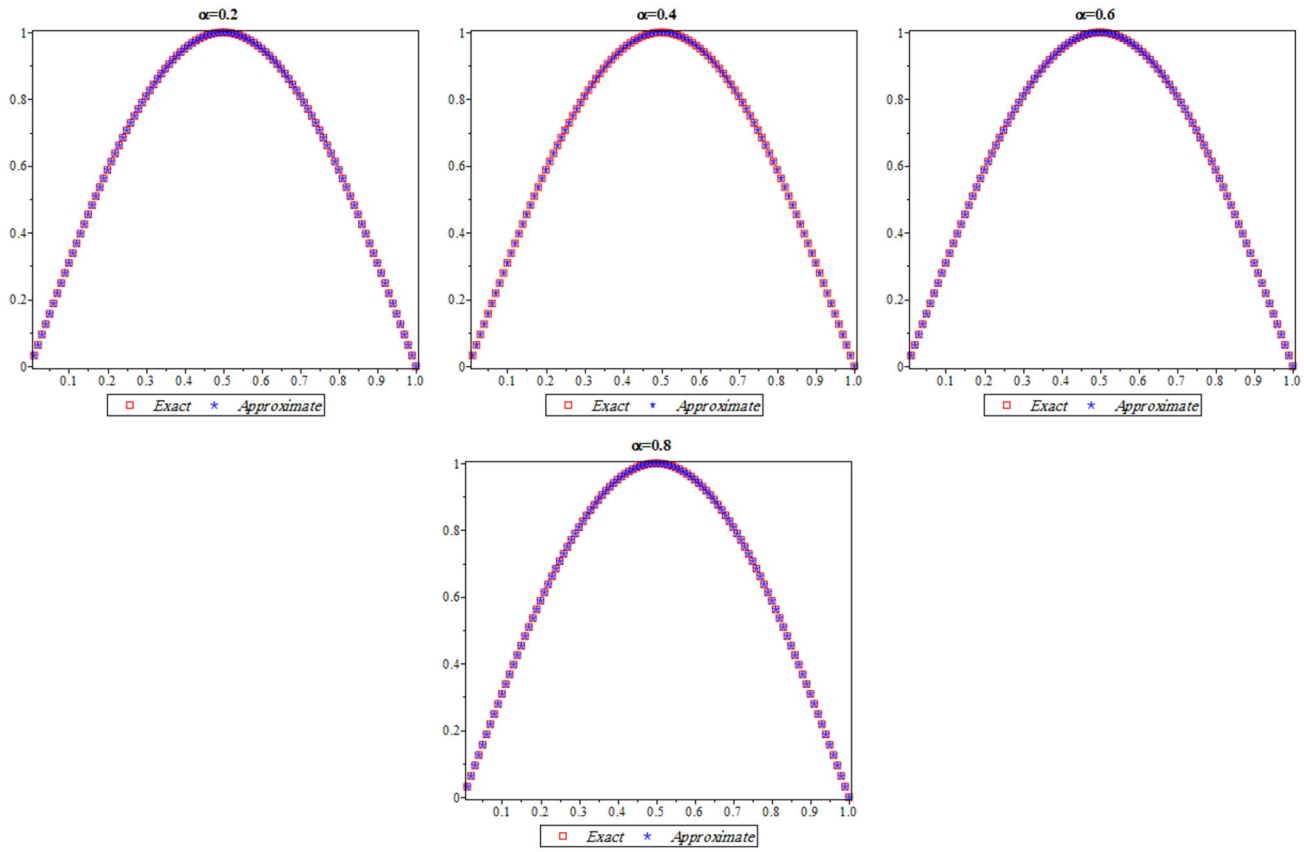

Fig. 1 Plots of the exact and numerical solutions at $T = 1$ with $h = \tau = \frac{1}{200}$ of Experiment 1

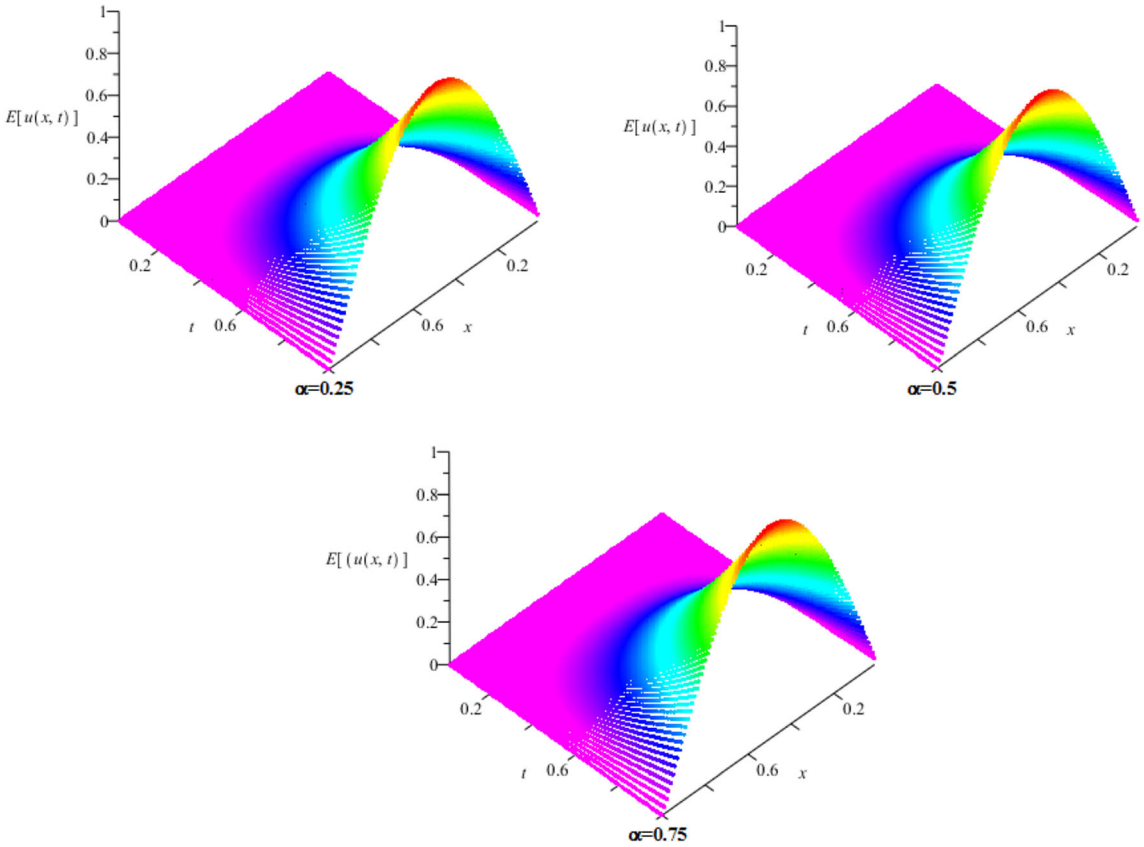

Fig. 2 Plots of the expected values E[u(x, t)] using the mean of 100 samples of Experiment 1

Table 4 Errors and CPU time in scheme (6) of Experiment 1

N	M	$\alpha = 0.25$	$\alpha = 0.5$	$\alpha = 0.75$
25	50	3.45×10^{-4}	4.05×10^{-4}	7.29×10^{-4}
		0.28 s	0.24 s	0.23 s
50	100	7.94×10^{-5}	6.04×10^{-5}	2.08×10^{-4}
		6.08 s	6.38 s	6.48 s
100	200	2.03×10^{-5}	1.06×10^{-4}	7.10×10^{-5}
		39.01 s	36.30 s	41.66 s

Table 5 Errors and CPU time in scheme (11) of Experiment 1

(N, G, m)	M	$\alpha = 0.25$	$\alpha = 0.5$	$\alpha = 0.75$
(25, 5, 4)	50	3.45×10^{-4}	4.05×10^{-4}	7.29×10^{-4}
		0.09 s	0.14 s	0.1 s
(50, 5, 4)	100	7.94×10^{-5}	6.04×10^{-5}	2.08×10^{-4}
		1.10 s	1.12 s	1.06 s
(100, 5, 4)	200	2.03×10^{-5}	1.06×10^{-4}	7.10×10^{-5}
		2.71 s	3.02 s	2.93 s

$$\|\widehat{u}^n - u^n\|_2 \le \sigma_{m+1}, \quad n = 1, 2, \ldots, G,$$

and

$$\|\widehat{u}^n - u^n\|_2 \le CL\sigma_{m+1}, \quad n = G+1, \ldots, N.$$

Proof Suppose $e^{*n} = \widehat{u}^n - u^n$. From (9), we get:

$$\|e^{*n}\|_2 = \|\widehat{u}^n - u^n\|_2 \le \sigma_{m+1}, \quad n = 1, 2, \ldots, G, \tag{17}$$

once $n = G+1, \ldots, N$, we replace u^n in (6) by $\widehat{u}^n$, then we obtain:

$$K_n \widehat{u}^n = \sum_{k=1}^{n-1} (a_{n-k-1} - a_{n-k})\widehat{u}^n + a_{n-1}\widehat{u}^0 + \mu F^n + B^n. \tag{18}$$

By subtracting (18) from (6) and utilizing the inner product with e^{*n}, we can obtain:

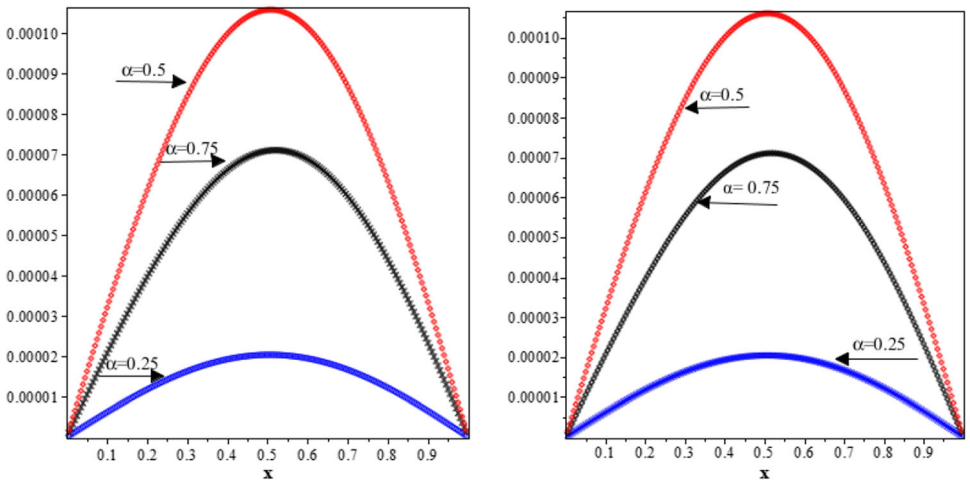

Fig. 3 The error curves RIFD (right) and IFD (left) schemes at $T = 1$ and $h = \tau = \frac{1}{200}$ of Experiment1

Table 6 Comparison of approximate and exact solutions with $h = \tau = \frac{1}{200}$ of Experiment 2

x	Exact	Approximate $\alpha = 0.2$	$\alpha = 0.4$	$\alpha = 0.6$	$\alpha = 0.8$
0.1	0.01326569	0.01326496	0.01327203	0.01327957	0.01254461
0.2	0.06819635	0.06819635	0.06821064	0.08822284	0.06688063
0.3	0.19186883	0.19185156	0.19187281	0.19188511	0.19039249
0.4	0.41611839	0.41608838	0.41611604	0.41612591	0.41512638
0.5	0.77573986	0.77569711	0.77572984	0.77574066	0.77543421
0.6	1.30589132	1.30583877	1.30587406	1.30589462	1.30592716
0.7	2.03897571	2.03891953	2.03895351	2.03899038	2.03930321
0.8	3.00114581	3.00109540	3.00112301	3.00117005	3.00218402
0.9	4.20868958	4.20865723	4.20867307	4.20870845	4.20996679

$$(K_n e^{*n}, e^{*n}) = \sum_{k=1}^{n-1}(a_{n-k-1} - a_{n-k})(K_n e^{*k}, e^{*n}), \quad n = G+1, \ldots, N.$$

From (12), the above equation can be rewritten as:

$$\|e^{*n}\|_2 \le \frac{1}{\lambda_{\min}(K_n)} \sum_{k=1}^{n-1}(a_{n-k-1} - a_{n-k})\|e^{*k}\|_2.$$

From Lemma 1, it follows that

$$a_{n-k-1} - a_{n-k} \le a_{n-k-1} < a_0 \le 1.$$

Now, from the above inequality and mathematical induction, we obtain:

$$\|e^{*n}\|_2 \le \sum_{k=1}^{n-1}\|e^{*k}\|_2 = \le \sum_{k=1}^{G}\|e^{*k}\|_2 + \sum_{k=G+1}^{n-1}\|e^{*k}\| \le G\sigma_{m+1} + \sum_{k=G+1}^{n-1}\|e^{*k}\|_2 \le CG\sigma_{m+1}.$$

Therefore, the theorem is proved.

Theorem 5 *By applying the assumptions of Theorem 4, suppose that* $\widehat{u}^n$ *be the solution vector of the RIFD scheme* (11) *and* u^n *be the solution vector of the IFD scheme*(6), *then*:

$$\|\widehat{u}^n - u^n\| \le \sigma_{m+1} + C(h^2 + \tau^{2-\alpha}), \quad n = 1, 2, \ldots, G,$$

and

$$\|\widehat{u}^n - u^n\| \le CG\sigma_{m+1} + C(h^2 + \tau^{2-\alpha}), \quad n = G+1, 2, \ldots, N,$$

here m is the number of POD bases.

6 Numerical Experiments

This section is devoted to implement two experiments. We illustrate the effectiveness of the RIFD scheme by the POD method. The programming code for simulating Wiener process over the interval [0, 1] has been given in Algorithm 1.

Algorithm 1. Simulating Wiener process.

$T = 1$

$\tau = \frac{T}{N}$

W=zeros$(N+1, 1)$;

for $n = 2$: $N + 1$

$W(n, 1) = W(n-1, 1) + \sqrt{\tau} * randn$;

To show the accuracy of the proposed scheme, we use the following error norm:

$$L_\infty = \max_{1 \le i \le M-1} |u(x_i, t_N - u_i^N|$$

We denote the numerical convergence orders by

Table 7 Numerical convergence orders in spatial direction with $\tau = \frac{1}{100}$ for Experiment 2

α	h	L_∞	$C_h - Order$
0.25	$\frac{1}{10}$	4.6029×10^{-3}	–
	$\frac{1}{20}$	1.1515×10^{-3}	1.9990
	$\frac{1}{40}$	2.8751×10^{-4}	2.0018
	$\frac{1}{80}$	7.1472×10^{-5}	2.0082
0.5	$\frac{1}{10}$	4.5830×10^{-3}	–
	$\frac{1}{20}$	1.4141×10^{-3}	2.0021
	$\frac{1}{40}$	2.8304×10^{-4}	2.0151
	$\frac{1}{80}$	6.7771×10^{-5}	2.0623
0.75	$\frac{1}{10}$	4.5396×10^{-3}	–
	$\frac{1}{20}$	1.1208×10^{-3}	2.0180
	$\frac{1}{40}$	2.6480×10^{-4}	2.0816
	$\frac{1}{80}$	5.0587×10^{-5}	2.3881

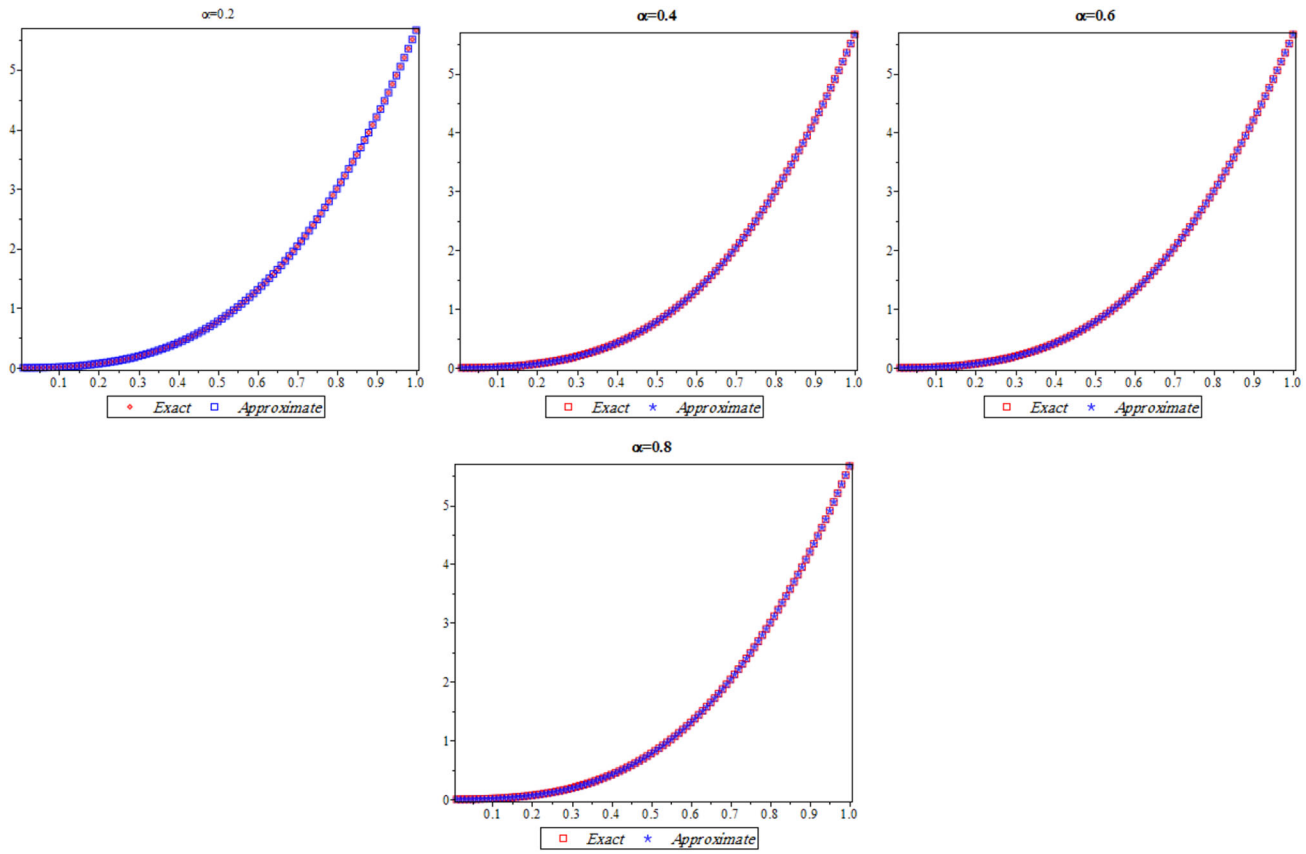

Fig. 4 Plots of the exact and approximate solutions at $T = 1$ and $h = \tau = \frac{1}{200}$ of Experiment 2

Table 8 Numerical convergence orders in temporal direction with $\alpha = 0.5$ and $h = \frac{1}{100}$ for Experiment 2

τ	L_∞	$C_\tau - Order$
$\frac{1}{8}$	5.4223×10^{-3}	–
$\frac{1}{16}$	1.7124×10^{-3}	1.6629
$\frac{1}{32}$	5.4333×10^{-4}	1.6561
$\frac{1}{64}$	2.2955×10^{-5}	1.2430

$$C_h - Order = \log_2\left(\frac{L_\infty(2h,\tau)}{L_\infty(h,\tau)}\right),$$
$$C_\tau - Order = \log_2\left(\frac{L_\infty(h,2\tau)}{L_\infty(h,\tau)}\right).$$

7 Experiment 1

Consider the FSA-DE in time as follows Mirzaee et al. 2020:

$$ {}_0^C\mathcal{D}_t^\alpha u(x,t) * = \left(\frac{1}{\pi^2} + \frac{dB(t)}{dt}\right)\frac{\partial^2 u(x,t)}{\partial x^2} + \frac{\partial u(x,t)}{\partial x} + f(x,t), \quad (x,t) \in (0,1)\times(0,1), \tag{19}$$

along with the initial and the boundary conditions, respectively:

$$u(x,0) = 0,$$
$$u(0,t) = 0,$$
$$u(1,t) = 0,$$

where $f(x,t) = \frac{2t^{2-\alpha}\sin(\pi x)}{\Gamma(3-\alpha)} + \left(\frac{1}{\pi^2} + \frac{\mathrm{dB}}{\mathrm{dt}}\right)\pi^2 t^2 \sin(\pi x) - \pi t^2 \cos(\pi x)$. $u(x,t) = t^2 \sin(\pi x)$ is considered as the exact solution.

Equation (19) is solved with the help of IFD scheme (6) with the $M, N = 100$ wherein exact and approximate solutions for different values of $\alpha = 0.2, 0.4, 0.6$ and 0.8 are tested. Table 1 confirms that the approximate solutions are close to exact solutions. It can be observed from Tables 2 and 3 that the numerical convergence orders are close to the theoretical orders. Figure 1 verifies the above mentioned solutions for values of $\alpha = 0.2, 0.4, 0.6$ and 0.8. Figure 2 shows the expected values E[u(x, t)] with different values α, $\alpha = 0.25, 0.5, 0.75$, where the expected values are computed by mean of 100 samples.

Table 9 Errors and CPU time in scheme (6) of Experiment 2

N	M	$\alpha = 0.25$	$\alpha = 0.5$	$\alpha = 0.75$
50	50	2.38×10^{-4}	3.58×10^{-4}	8.29×10^{-4}
		$4.82s$	$5.00s$	$5.14s$
100	100	1.70×10^{-5}	3.79×10^{-5}	3.69×10^{-5}
		$29.95s$	$27.18s$	$28.45s$

Table 10 Errors and CPU time in scheme (11) of Experiment 2

(N, G, m)	M	$\alpha = 0.25$	$\alpha = 0.5$	$\alpha = 0.75$
(50, 10, 6)	50	2.38×10^{-4}	3.58×10^{-4}	8.29×10^{-4}
		$2.15s$	$2.10s$	$1.81s$
(100, 11, 7)	100	1.70×10^{-5}	3.79×10^{-5}	3.69×10^{-5}
		$5.53s$	$5.64s$	$5.42s$

What extracts from Tables 4 and 5 is that in RIFD scheme the computational time is less than IFD scheme while the accuracy is preserved. The above tables confirm preference of the RIFD than IFD. Figure 3 shows this fact for $m = 4$ and $G = 7$.

8 Experiment 2

Consider the FSA-DE in time as follows Mirzaee et al. 2020:

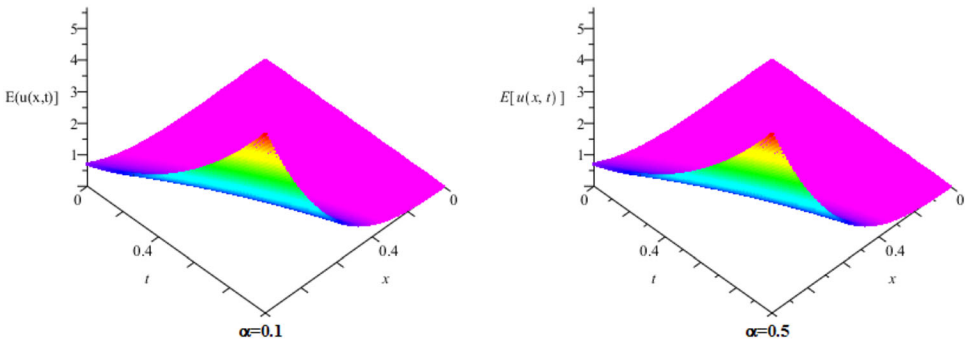

Fig. 5 Plots of the expected values E[u(x, t)] using the mean of 200 samples of Experiment 2

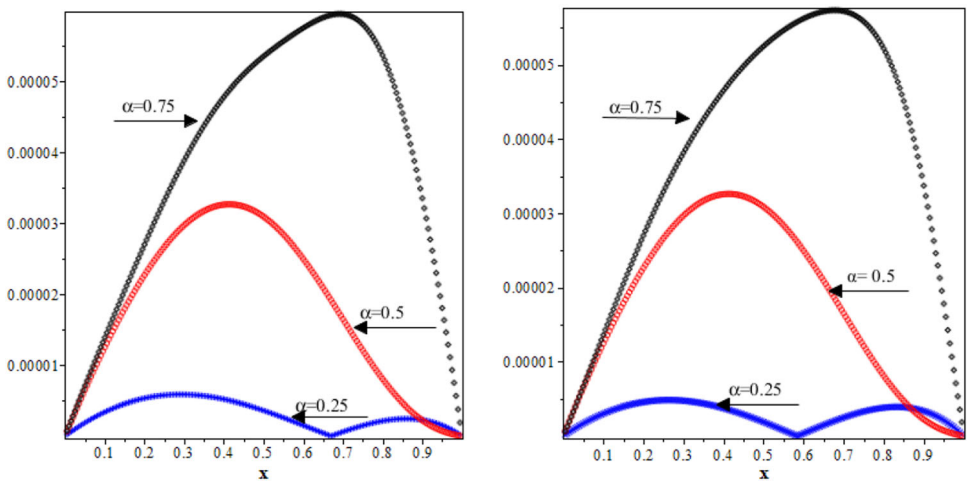

Fig. 6 The error curves RIFD (right) and IFD (left) schemes at $T = 1$ and $h = \tau = \frac{1}{200}$ of Experiment 2

$$
\begin{aligned}
{}_{0}^{C}\mathcal{D}_{t}^{\alpha}u(x,t) &= \left(1+\frac{dB(t)}{dt}\right)\frac{\partial^2 u(x,t)}{\partial x^2}+\frac{\partial u(x,t)}{\partial x} \\
&\quad +f(x,t), \quad (x,t)\in(0,1)\times(0,1),
\end{aligned} \tag{20}
$$

along with the initial and the boundary conditions, respectively:

$$
\begin{aligned}
&u(x,0) = x^3\sin^2(x),\\
&u(0,t) = 0,\\
&u(1,t) = (t+1)^3\sin^2(1).
\end{aligned}
$$

$u(x,t) = (t+x)^3\sin^2(x)$ is considered as the exact solution.

In Table 6, exact and approximate solutions for values of $\alpha = 0.2, 0.4, 0.6$ and 0.8 for $M, N = 100$ are tested. Table 4 confirms that the approximate solutions are close to exact solutions that this fact is shown in Fig. 4. Tables 7 and 8 show that the numerical convergence orders are compatible with the theoretical orders. Figure 4 verifies the above mentioned solutions for values of $\alpha = 0.2, 0.4, 0.6$ and 0.8. Figure 5 exhibits the expected values $\mathrm{E}[\mathrm{u}(\mathrm{x},\mathrm{t})]$ with different values $\alpha = 0.1$ and 0.5, where the expected values are computed by mean of 200 samples.

From Tables 9 and 10, we conclude that RIFD scheme is better than in sence that time taken is less compared with IFD scheme.

we exhibit the error curves for the IFD scheme in Fig. 6 with $h = t = \frac{1}{200}$ and $G = 11, m = 7$ for RIFD scheme which are observing alike.

9 Conclusions

In this article, we have benefitted from the POD technique to derive RIFD scheme for FSA-DE in order to make the proposed scheme better and useful than previous studies. The main features of the paper are to introduce a new scheme for FSA-DE in order to preserve accuracy and alleviate CPU time. We have tested the correctness of our scheme with two numerical experiments. Tables and figures confirm the efficiency of the presented scheme.

Acknowledgements The authors are very grateful to the reviewers for carefully reading the paper and for their comments and suggestions which have led to improvements of the paper.

Author Contributions ZS, AA and DB contributed to investigation; ZS, AA and DB contributed to writing—original draft preparation; ZS, AA and DB contributed to writing—review and editing. All authors have read and agreed to the published version of the manuscript.

Funding No funds, grants or other support were received.

Declarations

Conflict of interest The authors declare that they have no conflict of interest.

Ethical approval This article has not been published before; it is not under consideration for publication anywhere else.

References

Abbaszadeh M, Dehghan M (2020) A POD-based reduced-order Crank-Nicolson/fourth-order alternating direction implicit (ADI) finite difference scheme for solving the two-dimensional distributed-order Riesz space-fractional diffusion equation. Appl Numer Math 158:271–291

Abbaszadeh M, Dehghan M, Navon IM (2022) A POD reduced-order model based on spectral Galerkin method for solving the space-fractional Gray-Scott model with error estimate. Eng Comput 38:2245–2268

Abbaszadeh M, Dehghan M (2020) Reduced order modeling of time-dependent incompressible Navier-Stokes equation with variable density based on a local radial basis functions-finite difference (LRBF-FD) technique and the POD/DEIM method. Comput Methods Appl Mech Engrg 364:112914

Abedini N, Bastani AF, Zangeneh BZ (2021) Petrov-Galerkin finite element method using polyfractonomials to solve stochastic fractional differential equations. Appl Numer Math 169:64–86

Ciprian AT (2013) Analysis of variations for self-similar processes: a stochastic calculus approach. Springer, Berlin

Dehghan M, Abbaszadeh M (2018) A reduced proper orthogonal decomposition (POD) element free Galerkin (POD-EFG) method to simulate two-dimensional solute transport problems and error estimate. Appl Numer Math 126:92–112

Dehghan M, Abbaszadeh M (2018) An upwind local radial basis functions-differential quadrature (RBF-DQ) method with proper orthogonal decomposition (POD) approach for solving compressible Euler equation. Eng Anal Bound Elem 92:244–256

Dehghan M, Abbaszadeh M (2017) The use of proper orthogonal decomposition (POD) meshless RBF-FD technique to simulate the shallow water equations. J Comput Phys 351:478–510

Fu H, Wang H, Wang Z (2018) POD/DEIM reduced-order modeling of time-fractional partial differential equations with applications in parameter identification. J Sci Comput. https://doi.org/10.1007/s10915-017-0433-8

Gao GH, Sun ZZ, Zhang HW (2014) A new fractional numerical differentiation formula to approximate the Caputo fractional derivative and its applications. J Comput Phys 259:33–50

He JW, Peng L (2019) Approximate controllability for a class of fractional stochastic wave equations. Comput Math Appl 78:1463–1476

Holmes P, Lumley J, Berkooz G, Rowely CW (2012) Turbulence, coherent structures, dynamical systems and symmetry, 2nd edn. Cambridge University Press, Cambridge

Ren Q, Tian H (2022) Mean-square convergence and stability of two-step Milstein methods for stochastic differential equations with Poisson jumps. Comp Appl Math. https://doi.org/10.1007/s40314-022-01824-3

Horn RA, Johnson CR (1985) Matrix analysis. Cambridge University, Cambridge

Kamrani M (2015) Numerical solution of stochastic fractional differential equations. Numer. Algorithms. 68:81–93

Kunisch K, Volkwein S (2001) Galerkin proper orthogonal decomposition methods for parabolic problems. Numer Math 90:117–148

Kunisch K, Volkwein S (2002) Galerkin proper orthogonal decomposition methods for a general equation in fluid dynamics. SIAM J Numer Anal 40:492–515

Li F, Zhang S, Meng X (2019) Dynamics analysis and numerical simulations of a delayed stochastic epidemic model subject to a general response function. Comp Appl Math. https://doi.org/10.1007/s40314-019-0857-x

Liu J, Li H, Liu Y, Fang Z (2016) Reduced-order finite element method based on POD for fractional Tricomi-type equation. Appl Math Mech. https://doi.org/10.1007/s10483-016-2078-8

Liu X, Yang X (2021) Mixed finite element method for the nonlinear time-fractional stochastic fourth-order reaction-diffusion equation. Comput Math Appl 84:39–55

Yoon Y, Seo JH, Kim JH (2022) Closed-form pricing formulas for variance swaps in the Heston model with stochastic long-run mean of variance. Comput Appl Math 235:1–28

Luo Z, Chen G (2018) Proper orthogonal decomposition methods for partial differential equations. Academic Press, San Diego

Luo ZD, Chen J, Sun P, Yang X (2009) Finite element formulation based on proper orthogonal decomposition for parabolic equations. Sci China Ser A Math 52:587–596

Luo Z, Jin S, Chen J (2016) A reduced-order extrapolation central scheme based on POD for two-dimensional fourth-order hyperbolic equations. Appl Math Comput 289:396–408

Luo ZD, Ou QL, Wu JR, Xie ZH (2012) A reduced FE formulation based on POD for two-dimensional hyperbolic equation. Acta Math Sci 32:1997–2009

Luo ZD, Wang H (2020) A highly efficient reduced-order extrapolated finite difference algorithm for time-space tempered fractional diffusion-wave equation. Appl Math Lett 102:1–8

Luo ZD, Zhu J, Wang RW, Navon IM (2007) Proper orthogonal decomposition approach and error estimation of mixed finite element methods for the tropical pacific ocean reduced gravity model. Comput Meth Appl Mech Eng 196:4184–4195

Luo ZD, Zhou YJ, Yang X (2009) A reduced finite element formulation based on proper orthogonal decomposition for burgers equation. Appl Numer Math 59:1933–1946

Mirzaee F, Sayevand K, Rezaei S, Samadyar N (2020) Finite difference and spline approximation for solving fractional stochastic advection-diffusion equation Iran. J Sci Technol Trans Sci 45(2):607–617. https://doi.org/10.1007/s40995-020-01036-6

Oksendal B (2000) Stochastic differential equations. Springer, New York

Pedjeu JC, Ladde GS (2012) Stochastic fractional differential equations: modeling, method and analysis. Chaos, Solitons Fractals 45:279–293

Peng L, Huang Y (2019) On nonlocal backward problems for fractional stochastic diffusion equations. Comput Math Appl 78:1450–1462

Roth C (2002) Difference methods for stochastic partial differential equations. Z Angew Math Mech 82:821–830

Sakthivel R, Revathi P, Ren Y (2013) Existence of solutions for nonlinear fractional stochastic differential equations. Nonlinear Anal TMA 81:70–86

Sun P, Luo Z, Zhou Y (2010) Some reduced finite difference shcemes based on a proper orthogonal decomposition technique for parabolic equations. Appl Numer Math 60:154–164

Sweilam NH, El-Sakout DM, Muttardi MM (2020) Compact finite difference method to numerically solving a stochastic fractional advection-diffusion equation. Adv Differ Equ 189:1–20

Thomas JW (1995) Numerical partial differential equations: finite difference methods. Texts Appl. Math., Vol 22, Springer, New York

www.math.hkbu.edu.hk math lecture

Xu B, Zhang X (2019) An efficient high-order compact finite difference scheme based on proper orthogonal decomposition for the multi-dimensional parabolic equation. Adv Diff Equ 341:1–22

Zhang X, Zhang P (2018) A reduced high-order compact finite difference scheme based on proper orthogonal decomposition technique for KdV equation. Appl Math Comput 339:535–545

Zou G (2018) Galerkin finite element method for time-fractional stochastic diffusion equations. Comp Appl Math. https://doi.org/10.1007/s40314-018-0609-3

Zhou Y, Xie J, Zhang Z (2021) Highly efficient difference methods for stochastic space fractional wave equation driven by additive and multiplicative noise. Appl Math Lett 116:1–8

Zhuang P, Liu F (2006) Implicit difference approximation for the time fractional diffusion equation. J Appl Math Comput 22:87–99